ESC European Society of Cardiology

European Heart Journal - Case Reports (2023) **7**, 1–7
https://doi.org/10.1093/ehjcr/ytac491

CASE REPORT
Electrophysiology

Additional left ventricular septal lead facilitates R-wave sensing of implantable cardioverter-defibrillator in arrhythmogenic right ventricular cardiomyopathy: a case report

Wenzhao Lu, Keping Chen *, Yan Dai, and Shu Zhang

State Key Laboratory of Cardiovascular Disease, Arrhythmia Center, Fuwai Hospital, National Center for Cardiovascular Diseases, Chinese Academy of Medical Sciences & Peking Union Medical College, No. 167, Beilishi Road, Xicheng District, Beijing 100037, China

Received 1 August 2022; first decision 12 August 2022; accepted 30 December 2022; online publish-ahead-of-print 4 January 2023

Background Implantable cardioverter-defibrillator (ICD) implantation is a key therapeutic option in arrhythmogenic right ventricular cardiomyopathy (ARVC) to prevent sudden cardiac death due to ventricular tachycardia (VT) and fibrillation (VF). However, sub-optimized R-wave sensing due to myocardium loss interferes with VT/VF identification and appropriate therapy. We tried to implant a 3830 lead to the left ventricular septum (LVS) to facilitate ICD sensing in an ARVC patient.

Case summary A 68-year-old woman diagnosed with ARVC was scheduled to undergo ICD implantation. Initially, no sites with suitable R-wave amplitudes were found in the right ventricle (RV) to deploy the defibrillation lead (<3.0 mV). It was likely due to severe RV involvement, but the LVS myocardium was more preserved based on cardiac magnetic resonance imaging. Therefore, we implanted a 3830 lead into the deep area of the septum to facilitate R-wave sensing. During the procedure from the right to left septum, the R-wave amplitude significantly increased (2.6 to 4.3–7.1 mV). Left ventricular septum pacing was finally achieved with favourable R-wave sensing (9.9 mV 24 h post-operation). The 3830 lead was plugged into the IS-1 port, while the defibrillation lead was plugged into the DF-1 port. After a 4-month follow-up, the R-wave amplitude of the 3830 lead was 11.1 mV.

Discussion When the R-wave sensing is not acceptable for ICD implantation in ARVC patients, it is critical to assess myocardial conditions comprehensively. If the septal myocardium is preserved, implanting a 3830 lead to the deep or LVS is feasible to improve R-wave sensing.

Keywords Arrhythmogenic right ventricular cardiomyopathy • Implantable cardioverter-defibrillator • R-wave sensing • left ventricular septal pacing • Case report

ESC Curriculum 5.10 Implantable cardioverter defibrillators • 5.6 Ventricular arrhythmia • 6.7 Right heart dysfunction • 6.5 Cardiomyopathy

* Corresponding author. Tel: +86 10 8832 2295, Fax: 010 8832 2295, Email: chenkeping@263.net
Handling Editor: Robert Schönbauer
Peer-reviewers: Peregrine Green; Ugur Canpolat
Compliance Editor: Zhiyu Liu
Supplementary Material Editor: Gonçalo Costa

Learning points

- For arrhythmogenic right ventricular cardiomyopathy (ARVC) patients with extensive right ventricle (RV) lesions, conventional defibrillation lead may be unable to reach favourable R-wave sensing in RV, potentially influencing the detection of ventricular arrhythmias.
- Before implantable cardioverter-defibrillator (ICD) implantation in ARVC patients, the comprehensive evaluation of the preserved myocardium, such the cardiac magnetic resonance imaging, helps predict the lead's sensing performance.
- Implanting a 3830 lead to the deep or left ventricular septum is a feasible way to solve the poor RV R-wave sensing problem when implanting ICD devices in ARVC patients with preserved septal myocardium.

Introduction

Arrhythmogenic right ventricular cardiomyopathy (ARVC) is a heritable myocardial disease with high risk of life-threatening ventricular arrhythmias (VAs) and sudden cardiac death (SCD).[1,2] ARVC is characterized by fibrofatty replacement of functional myocardium dominantly in the right ventricle (RV), causing arrhythmogenic substrates and ventricular dysfunction.[3] Implantable cardioverter-defibrillator (ICD) is effective in preventing SCD in ARVC due to sustained ventricular tachycardia (VT) or fibrillation (VF).[4] However, progressive myocardium loss deteriorates the defibrillation lead's sensing ability, causing unsuccessful or inappropriate delivery of ICD therapy and even death.[5] A case report has demonstrated the feasibility of a trans-coronary sinus (trans-CS) left ventricular (LV) lead in improving ICD's R-wave sensing.[6] In recent years, left bundle branch area pacing (LBBAP) was popularized, including left bundle branch pacing and left ventricular septal pacing (LVSP).[7] It is achieved by a trans-septal lead screwed from the right to the left side of the ventricular septum, capturing the LV septal (LVS) myocardium or left bundle branch fibres. We present hereby an ARVC patient receiving an LVSP lead to enhance the R-wave sensing of ICD.

Timeline

Time	Event
Around 2010 (aged 58 years)	Gradually developed post-exertion dyspnoea, faintness, palpitation, and paroxysmal nocturnal dyspnoea.
January, 2020	Suspected arrhythmogenic right ventricular cardiomyopathy (ARVC) based on echocardiography and Holter electrocardiography (ECG; premature ventricular contraction and ventricular tachycardia episodes). Began anti-heart failure medication therapy.
31 December 2021	Spontaneous palpitation with a self-measured heart rate of ≈180 b.p.m. accompanied by a subsequent episode of syncope with tachycardia for about 1 min without documented ECG. Afterwards, two additional attacks occurred.
28 February 2022	The patient was admitted to our hospital, diagnosed with ARVC, and scheduled to receive an implantable cardioverter-defibrillator (ICD).
8 March 2022	The first attempt to implant a conventional dual-chamber ICD was performed. Poor R-wave sensing in right ventricle was found and the procedure was abandoned.
10 March 2022	The second attempt to implant an additional 3830 lead to the left ventricular septum to facilitate R-wave sensing was performed. The bipolar R-wave amplitudes of 5.8 and 9.9 mV were achieved at implantation and 24 h post-operation, respectively.
12 July 2022	The bipolar R-wave amplitude of the 3830 lead was 11.1 mV. Other parameters were maintained stable.

Case presentation

A 68-year-old woman was admitted to our hospital complaining of heart palpitation and syncope episodes accompanied by tachycardia (around 180 b.p.m.). She gradually developed post-exertion dyspnoea and faintness 10 years ago. Physical examination revealed blunt heart sound and systolic murmur at the tricuspid auscultation area. Serum N-terminal pro-brain natriuretic peptide (NT-proBNP) was 899.0 pg/mL. Electrocardiography (ECG) showed incomplete right bundle branch delay, inverted T waves in V1–V6 ECG leads, generally low QRS amplitude, and an Epsilon wave in V1 lead (*Figure 3A*). Echocardiography revealed a dilated RV (41 mm) and a reduced fractional area change (26%). Cardiac magnetic resonance imaging (CMRI) further confirmed RV enlargement, reduced RV ejection fraction (25.88%), increased RV end-diastolic volume index (235.48 mL/m^2), and extensive late gadolinium enhancement (LGE) in RV as a sign of fibrofatty replacement (*Figure 1A* and *B*; see Supplementary material online, *Video S1*). The LV and septum were more preserved. Other results and details are provided in *Table 1*.

According to the Modified Criteria,[4] the diagnosis of ARVC was established and a dual-chamber ICD was considered for the high VT/VF risk. During the procedure, the defibrillation lead (Boston Scientific, Model 0673) was primarily located at the middle RV septum (RVS), where the bipolar R-wave amplitude was low (around 2.0 mV). Then different sites were tried, including the anterior, posterior, and basal septum, the RVOT, and the apex, but the R-wave amplitude was generally low (< 3.0 mV), not satisfying the criteria to deploy a defibrillation lead.[8] Therefore, the operation was abandoned. Poor R-wave sensing was likely due to extensive RV lesions.

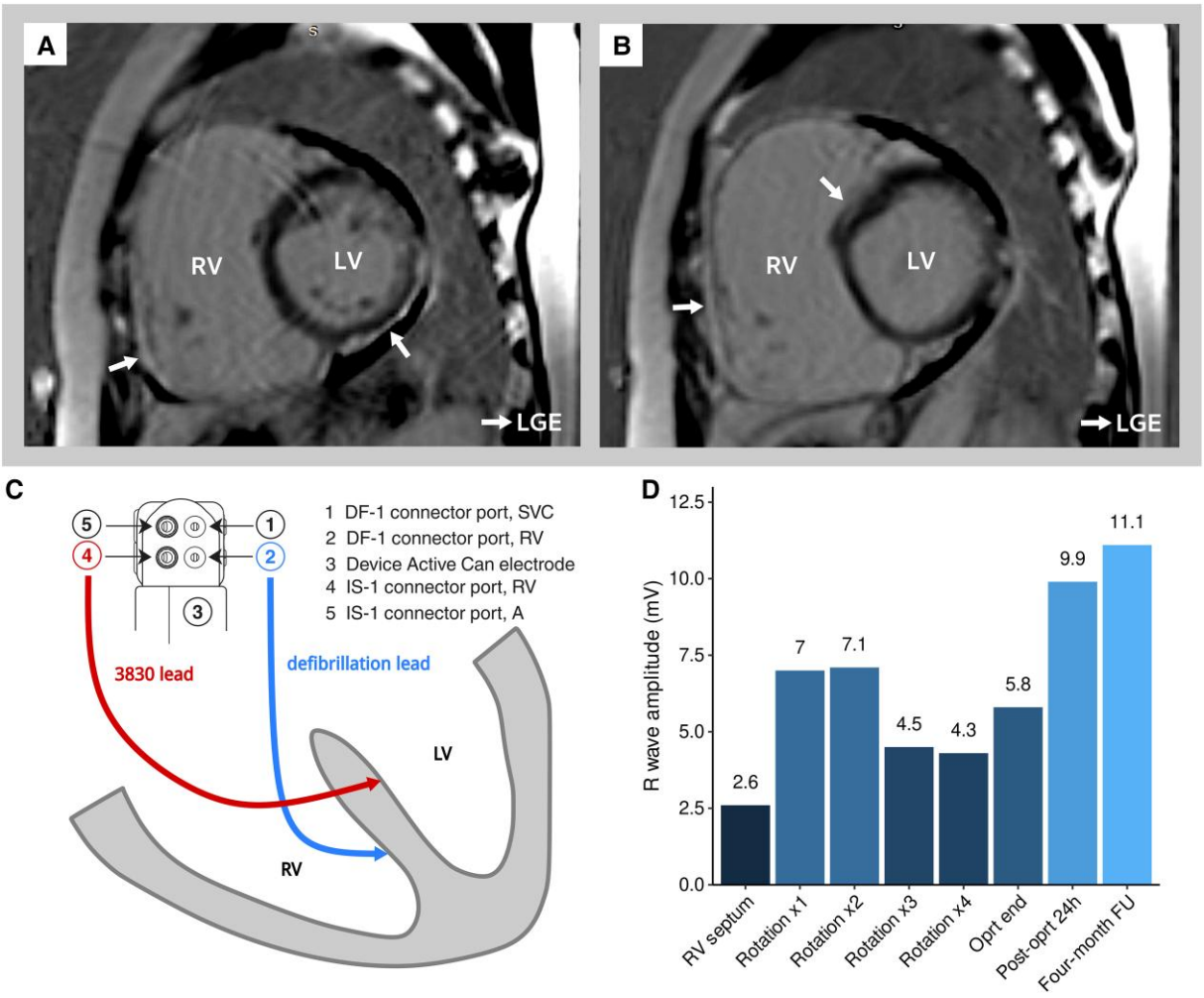

Figure 1 (*A* and *B*) Cardiac magnetic resonance imaging demonstrates right ventricle enlargement and late gadolinium enhancement at extensive right ventricle free wall, right ventricle septal–endocardial, and left ventricular lateral–subepicardial areas. (*C*) The strategy to screw a 3830 lead to the left ventricular septum and plug it into the right ventricle pacing/sensing port (IS-1) while plugging the defibrillation lead into the defibrillation port (DF-1). (*D*) Bipolar R-wave amplitude at the final site during lead implantation, post-operation test, and follow-up. Rotation ×1–4, the first to the fourth rounds of lead rotation. Oprt end, at the operation end; Post-oprt 24 h, 24 h post-operation; FU, follow-up.

Since the LVS myocardium was more preserved, a strategy was proposed to screw a 3830 lead (SelectSecure™, Medtronic) to the deep or left septum and plug it into the RV pacing/sensing port (IS-1) to enhance the R-wave sensing, while still plugging the defibrillation lead into the defibrillation port (DF-1) (*Figure 1C*). Accordingly, the second operation was performed. The 3830 lead was located at the RVS via the C315HIS sheath (Medtronic), recording the bipolar R-wave amplitude ranging from 1.5 to 2.8 mV. At the final targeted site, the bipolar R-wave amplitude sharply elevated from 2.6 to 7.1 mV after the first two rounds of rotation, then decreased to 4.3 mV after successive two rotations but slightly recovered to 5.8 mV at the end (*Figure 1D*). During the procedure, the unipolar paced QRS morphology and stimulus-to-left ventricular activation time (stim-LVAT) were monitored; LBB potential was recorded (*Figure 2*). Left ventricular septal pacing was eventually defined without documenting the direct evidence of LBB capture. Subsequently, the defibrillation lead (Model 6935, Medtronic) was deployed at the RVS. We chose a DF-1 dual-chamber ICD (Evera™, Model DDBC3D1, Medtronic), plugging the 3830 lead into the RV IS-1 port and the 6935 lead into the DF-1 port. The IS-1 end of the 6935 lead was embedded at the pocket bottom. Final lead positions are shown in *Figure 3B–D*.

Device programming 24 h post-operation demonstrated a favourable performance of both 3830 (R-wave = 9.9 mV; impedance = 551 Ω; threshold = 0.5 V/0.4 ms) (*Figure 1D*) and 6935 (defibrillation impedance = 53 Ω) leads (*Table 2*). Paced QRS is shown in *Figure 3A*. Echocardiography demonstrated that the intra-septal depth of the 3830 lead tip was 6.83 mm, around 1.0 mm from the LVS endocardium (*Figure 3E*). The patient was discharged with the ICD therapy settings and medications as shown in *Table 2*. After a 4-month follow-up, the parameters of both 3830 (R-wave = 11.1 mV) (*Figure 1D*) and 6935 (defibrillation impedance = 64 Ω) leads were stable, detecting 246 short VT episodes (<188 b.p.m.) accompanied by mild palpitation and dyspnoea without inappropriate delivery and device-related complications or adverse events (*Table 2*). Radiofrequency ablation was not considered due to low patient willingness and limited efficacy.

Table 1 Baseline clinical parameters

Clinical parameters	Values	Normal ranges
Laboratory test		
NT-proBNP (pg/mL)	899.0	<150
Albumin (g/L)	42.3	40–55
Blood urea nitrogen (mmol/L)	20.89	2.86–7.90
Creatinine (μmol/L)	166.71	44–133
Electrocardiography (ECG)		
QRS duration (ms)	114	60–110
Epsilon wave	Yes (V1 ECG lead)	None
Inverted T wave (precordial lead)	Yes (V1–6 ECG leads)	Upward T wave
Low QRS amplitude	Yes (except V2 ECG leads)	R + S > 0.5 mV
Holter ECG	14 874 PVC 4 short VT episodes	<100 PVC/24 h
Echocardiography		
RA diameter (mm)	44	29–45
RV diameter (mm)	41	19–35
RVFAC (%)	26	> 40
TAPSE (mm)	17	> 17
Tricuspid regurgitation	Moderate–severe	None
LVESD (mm)	37	22–35
LVEDD (mm)	50	38–52
LV ejection fraction (%)	55	54–74
Interventricular septum (mm)	8	6–10
Mitral regurgitation	Mild	None
RV segmental akinesia	Yes	None
Thin RV wall (mm)	2.0	2.2–6.2
CMRI		
RA diameter (mm)	58	24–59
RV diameter (mm)	44	15–34
RVOT (mm)	46	21–35
RV paradoxical movement	Yes	None
RV ejection fraction (%)	25.88	51–71
RVEDVi (mL/m^2)	235.48	51–97
Late gadolinium enhancement (fibrofatty infiltration)	RV: transmural LV: apex/lateral–subepicardial IVS: right-side subendocardial	None

NT-proBNP, N-terminal pro-brain natriuretic peptide; PVC, premature ventricular contraction; VT, ventricular tachycardia; RA, right atrial; RV, right ventricular; RVFAC, right ventricular fractional area change; TAPSE, tricuspid annular plane systolic excursion; LVESD, left ventricular end-systolic diameter; LVEDD, left ventricular end-diastolic diameter; RVOT, right ventricular outflow tract; RVEDVi, right ventricular end-diastolic volume index.

Discussion

As the foundation of appropriate ICD therapies, the correct and timely identification of VT/VF is based on sufficient ventricular sensing. Since the defibrillation test is now not regularly performed at ICD implantation, VA sensing is predicted by the R-wave amplitude in sinus rhythm. A study[8] found a positive correlation in amplitude between the R-wave in sinus rhythm and the F-wave during VF; it recommended the bipolar R-wave amplitude of ≥3.0 mV to ensure reliable VF detection. Moreover, poor R-wave sensing requires higher sensitivity, potentially increasing oversensing and inappropriate ICD therapy.[9] In ARVC, progressive myocardium loss causes significant deterioration in R-wave sensing and defects in VT/VF detection.[5,10] Taleski *et al.*[6] have implanted a trans-CS LV lead to enhance the ICD sensing in an ARVC patient, but it is challenging due to right heart enlargement and unstable contact with the epicardial myocardium to maintain sufficient R-wave sensing. In contrast, LBBAP was confirmed to produce more stable and excellent performance.[7]

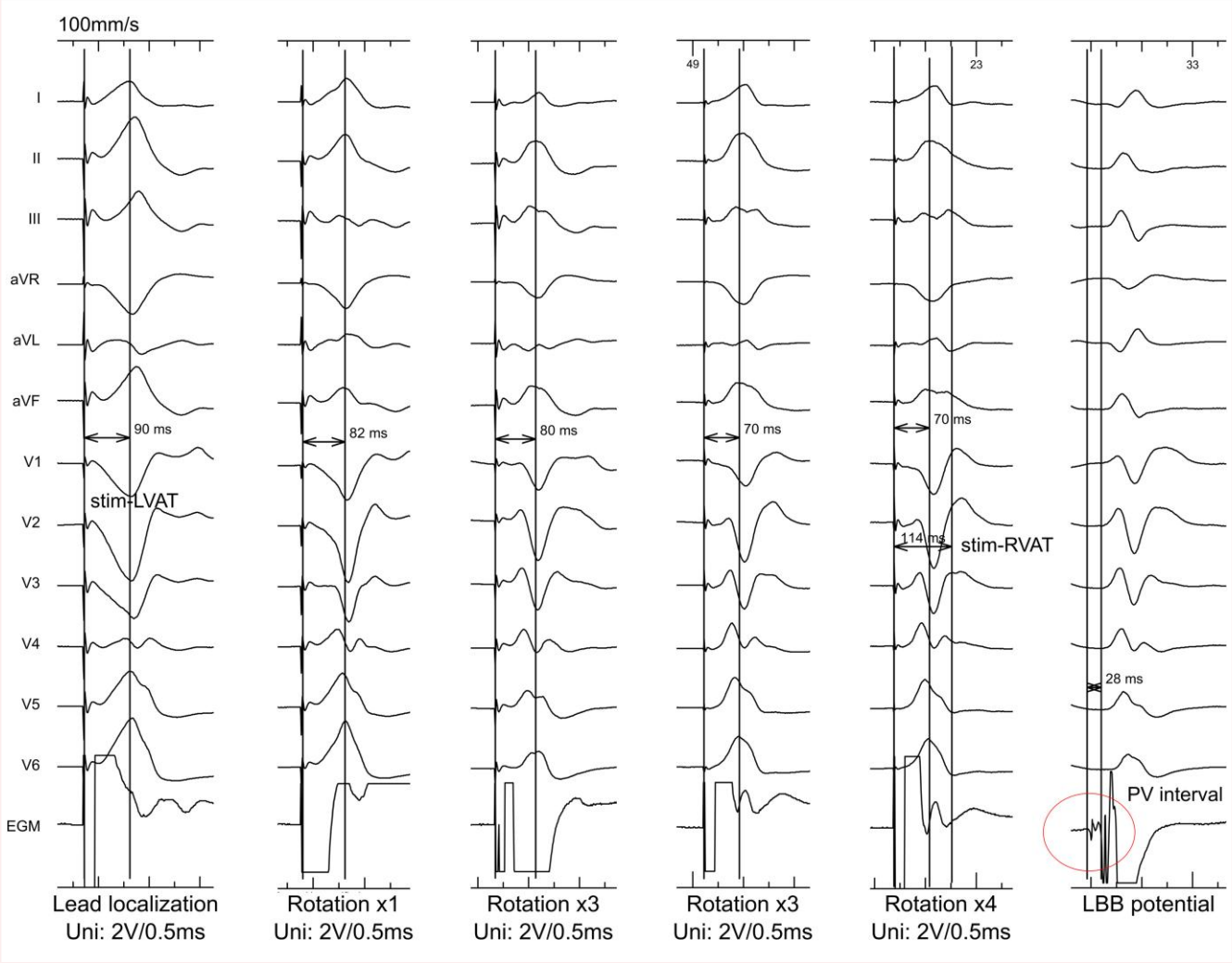

Figure 2 Paced QRS (100 mm/s, unipolar) during 3830 lead implantation and the left bundle branch potential. The stimulus-to-left ventricular activation time was gradually shortened as the lead moved forward. The V1–V6 inter-peak interval was 44 ms (stimulus-to-right ventricular activation time —stimulus-to-left ventricular activation time). The potential-to-ventricular activation interval was 28 ms, corresponding to that reported in left bundle branch area pacing.

In this case, no sites in RV with ideal R-wave amplitude were initially identified to deploy the defibrillation lead likely due to extensive RV lesions. Cardiac magnetic resonance imaging revealed the more preserved LV and septal myocardium, the characteristic of ARVC due to desmosomal mutations and severer myocardial uncoupling in RV in response to elevated afterload and wall stress.[1] Consequently, it was rational to screw a 3830 lead to the deep septal area to find a site with preserved myocardium. During screwing the lead, the R-wave amplitude was significantly increased after the initial rotations with subsequent decline likely due to acute myocardial injury. Implantable cardioverter-defibrillator test post-operation and after follow-up revealed favourable R-wave sensing and also other parameters. This result corresponded to what the CMRI found, indicating the importance of comprehensive myocardium evaluation before ICD implantation in ARVC patients. Moreover, studies[11,12] have demonstrated the value of electroanatomical and voltage mapping (EAVM) in assessing the abnormal myocardial substrate colocalized with LGE areas in ARVC, mainly reflecting the status of endocardial or epicardial myocardium and the intramural or septum areas. Hence, EAVM is valuable in evaluating appropriate sites before device implantation as a complement to CMRI. Left bundle branch area pacing (LVSP) was easily achieved in the case, but it is unnecessary to pursue LBBAP in this population. A deep septal area with preserved myocardium and favourable R-wave sensing is the target.

Conclusion

We first reported an ARVC patient receiving an LVSP lead with a defibrillation lead to facilitate ICD sensing. This strategy is practical to solve the situation of poor RV sensing in ARVC patients with extensive RV lesions but preserved septal myocardium, which requires further confirmation.

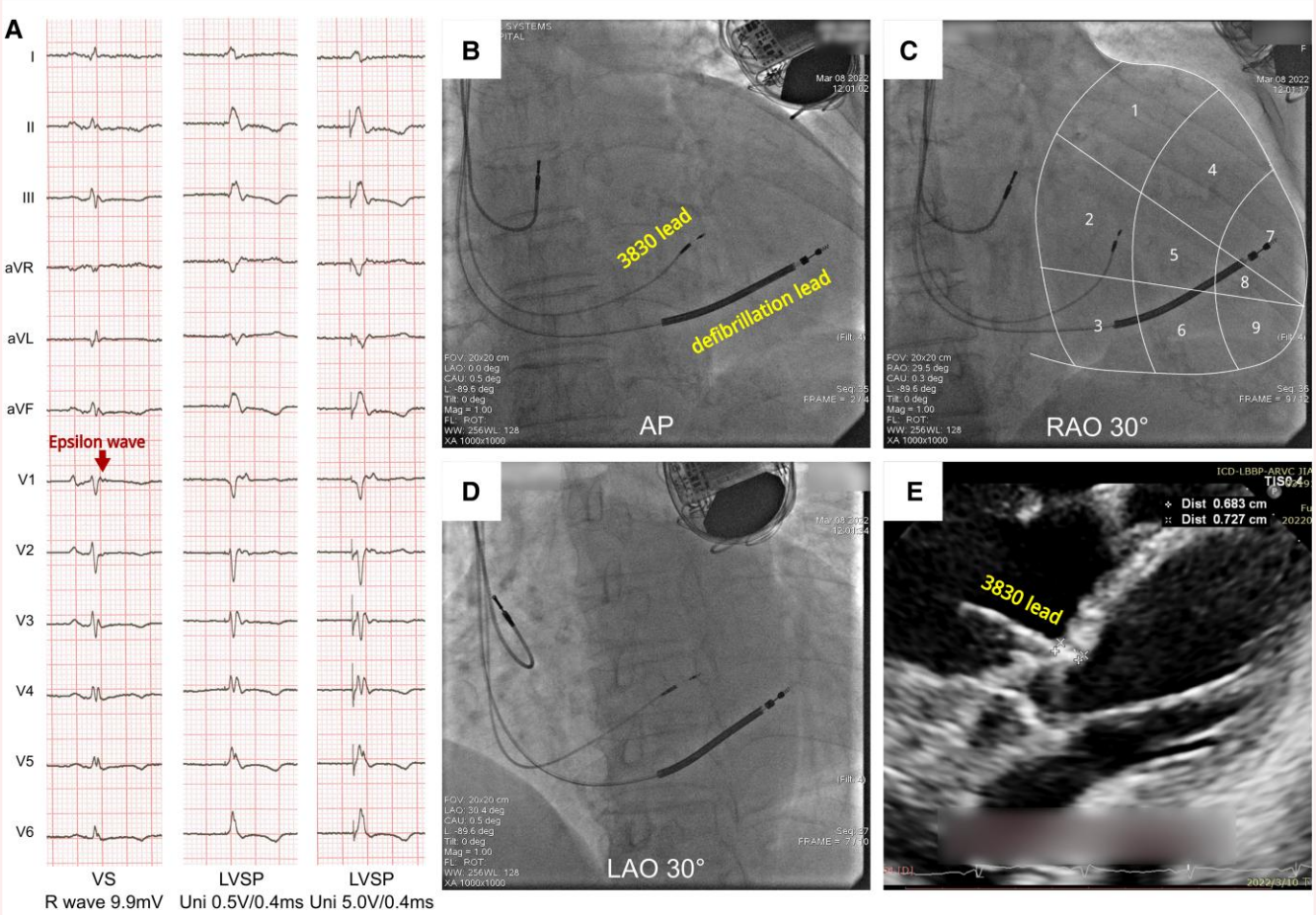

Figure 3 (*A*) Post-implantation intrinsic and paced electrocardiography (25 mm/s); epsilon wave could be seen in V1 lead during sinus rhythm, with the bipolar R-wave amplitude of 9.9 mV; similar paced QRS and stimulus-to-left ventricular activation time at low and high pacing outputs. (*B*) The final lead positions in an anteroposterior fluoroscopic view. (*C*) The final lead positions in right anterior oblique (RAO) 30° fluoroscopic view with the novel nine-partition method, showing that the 3830 lead was deployed in the most common implanted site of left bundle branch area pacing (junction of the 2nd and 5th partitions). (*D*) The final lead positions in left anterior oblique (LAO) 30° fluoroscopic view. (*E*) The intra-septal depth of the 3830 lead measured by echocardiography. EGM, electrogram; VS, ventricular sensing during sinus rhythm; LVSP, left ventricular septal pacing; Stim-LVAT, stimulus-to-left ventricular activation time.

Table 2 Implantable cardioverter-defibrillator programming parameters and medications

Parameters	Values
24 h post-implantation	
RV sensing (3830 lead, mV)	9.9
RV pacing threshold (V/0.4 ms)	0.5
Pacing impedance (Ω)	551
Defibrillation impedance (Ω)	53
ICD therapy setting	
AT/AF	> 171 b.p.m., monitor only
VT	Off
FVT	Off
VF	>188 b.p.m., monitor, ATP during charging, 35J*6
Four-month follow-up	
RV sensing (3830 lead, mV)	11.1
RV pacing threshold (V/0.4 ms)	0.5
Pacing impedance (Ω)	513
Defibrillation impedance (Ω)	64
AP, VP (%)	43.4, 0.1
VT	133–188 b.p.m., 246 episodes
AT/AF	13 episodes
Longest AT/AF duration (min)	26
ICD therapy	None
Medications	
Bisoprolol	1.25 mg, q.d.
Atorvastatin	20 mg, q.d.
Furosemide	10 mg, q.d.
ARNI (sacubitril/valsartan)	100 mg, b.i.d.

AT/AF, atrial tachycardia/fibrillation; VT, ventricular tachycardia; FVT, fast VT; VF, ventricular fibrillation; RV, right ventricular; AP, atrial pacing percentage; VP, ventricular pacing percentage; ATP, anti-tachycardia pacing; ARNI, angiotensin receptor-neprilysin inhibitor; q.d., once a day (quaque die); b.i.d., twice a day (bis in die).

Lead author biography

Dr Keping Chen gained her doctorate of medicine from Peking Union Medical College, Beijing, China and is now working as a director in the Arrhythmia Center of Fuwai Hospital. She specializes in cardiac pacing and electrophysiology with more than 20-year experience in arrhythmia management and device therapy. She serves as one of the general secretary of the committee of the cardiac electrophysiology and pacing branch of the Chinese Medical Association.

Supplementary material

Supplementary material is available at *European Heart Journal – Case Reports* online.

Acknowledgements

We thank Dr Ruohan Chen for patient management; Dr Zhongli Chen for collecting and analysing CMRI images; Dr Nan Xu for echocardiography examination; and Dr Yao Li for patient follow-up. They all work in Fuwai Hospital.

Slide sets: A fully edited slide set detailing this case and suitable for local presentation is available online as Supplementary data.

Consent: The authors confirm that written consent for the submission and publication of this case, including images, has been obtained from the patient in line with COPE guidance.

Conflict of interest: The authors declare no conflicts of interest.

Funding: Not available.

Data availability

The data underlying this article cannot be shared publicly due to the data confidentiality policy of the National Center for Cardiovascular Diseases (China).

References

1. Corrado D, Link MS, Calkins H. Arrhythmogenic right ventricular cardiomyopathy. *N Engl J Med* 2017;**376**:61–72.
2. Gandjbakhch E, Redheuil A, Pousset F, Charron P, Frank R. Clinical diagnosis, imaging, and genetics of arrhythmogenic right ventricular cardiomyopathy/dysplasia: JACC state-of-the-art review. *J Am Coll Cardiol* 2018;**72**:784–804.
3. Hoorntje ET, Te Rijdt WP, James CA, Pilichou K, Basso C, Judge DP, *et al.* Arrhythmogenic cardiomyopathy: pathology, genetics, and concepts in pathogenesis. *Cardiovasc Res* 2017;**113**:1521–1531.
4. Towbin JA, McKenna WJ, Abrams DJ, Ackerman MJ, Calkins H, Darrieux FCC, *et al.* 2019 HRS expert consensus statement on evaluation, risk stratification, and management of arrhythmogenic cardiomyopathy. *Heart Rhythm* 2019;**16**:e301–e372.
5. Sagawa Y, Nagata Y, Yamaguchi T, Mitsui K, Nagamine T, Yamaguchi J, *et al.* Long-term performance of right ventricular implantable cardioverter-defibrillator leads in arrhythmogenic right ventricular cardiomyopathy and hypertrophic cardiomyopathy. *Int Heart J* 2020;**61**:39–45.
6. Taleski J, Manola Š, Radeljić V, Bulj N, Delić Brkljačić D, Pavlović N. Left ventricular lead placement for pacing and sensing in a patient with arrhythmogenic right ventricular cardiomyopathy undergoing ICD implantation. *Acta Clin Croat* 2019;**58**:391–393.
7. Huang W, Zhou X, Ellenbogen KA. Pursue physiological pacing therapy: a better understanding of left bundle branch pacing and left ventricular septal myocardial pacing. *Heart Rhythm* 2021;**18**:1290–1291.
8. Ruetz LL, Koehler JL, Brown ML, Jackson TE, Belk P, Swerdlow CD. Sinus rhythm R-wave amplitude as a predictor of ventricular fibrillation undersensing in patients with implantable cardioverter-defibrillator. *Heart Rhythm* 2015;**12**:2411–2418.
9. Watanabe H, Chinushi M, Izumi D, Sato A, Okada S, Okamura K, *et al.* Decrease in amplitude of intracardiac ventricular electrogram and inappropriate therapy in patients with an implantable cardioverter defibrillator. *Int Heart J* 2006;**47**:363–370.
10. Herman ARM, Gardner M, Steinberg C, Yeung-Lai-Wah JA, Healey JS, Leong-Sit P, *et al.* Long-term right ventricular implantable cardioverter-defibrillator lead performance in arrhythmogenic right ventricular cardiomyopathy. *Heart Rhythm* 2016;**13**:1964–1970.
11. Hoogendoorn JC, Sramko M, Venlet J, Siontis KC, Kumar S, Singh R, *et al.* Electroanatomical voltage mapping to distinguish right-sided cardiac sarcoidosis from arrhythmogenic right ventricular cardiomyopathy. *JACC Clin Electrophysiol* 2020;**6**:696–707.
12. Andrews CM, Srinivasan NT, Rosmini S, Bulluck H, Orini M, Jenkins S, *et al.* Electrical and structural substrate of arrhythmogenic right ventricular cardiomyopathy determined using noninvasive electrocardiographic imaging and late gadolinium magnetic resonance imaging. *Circ Arrhythm Electrophysiol* 2017;**10**:e005105.